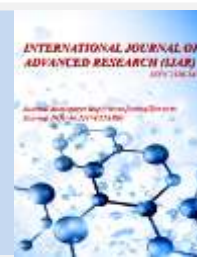




Journal Homepage: - www.journalijar.com
**INTERNATIONAL JOURNAL OF
 ADVANCED RESEARCH (IJAR)**

Article DOI: 10.21474/IJAR01/5124
 DOI URL: <http://dx.doi.org/10.21474/IJAR01/5124>



RESEARCH ARTICLE

NANOSTRUCTURED $\text{Ni}_{0.9}\text{Co}_{2.1}\text{O}_4$ SPINEL OXIDE: ELECTROCHEMICAL, SPECTROSCOPIC AND MORPHOLOGICAL INVESTIGATION.

Mamadou Guèye¹, Papa Charles Harris Mandiamy¹, * Makhtar Guène¹ and Abdou Aziz Diagne².

1. Laboratoire de Chimie Physique Organique et d'Analyse Environnementale, Département de Chimie, Faculté des Sciences et Techniques, Université Cheikh Anta Diop, Dakar, Sénégal.
2. Département de chimie, UFR SATIC, Université Alioune Diop, Bambey, Sénégal.

Manuscript Info

Manuscript History

Received: 10 June 2017
 Final Accepted: 12 July 2017
 Published: August 2017

Key words:-

Nanostructured $\text{Ni}_{0.9}\text{Co}_{2.1}\text{O}_4$, sol-gel, morphological, optical, electrochemical properties .

Abstract

Nickel cobalt oxide $\text{Ni}_{0.9}\text{Co}_{2.1}\text{O}_4$ powder were prepared by sol-gel via propionic acid technique from mixed aqueous solutions of hydrated cobalt nitrate ($\text{Co}(\text{NO}_3)_2 \cdot 6\text{H}_2\text{O}$) and hydrated nickel nitrate ($\text{Ni}(\text{NO}_3)_2 \cdot 6\text{H}_2\text{O}$) as sources of cobalt and nickel respectively. The system evolves toward the formation of the spinel phase, with further temperature thermal treatment at 350 °C. The structural, morphological, optical and electrochemical properties of the synthesized products were characterized through several techniques including ultraviolet-visible spectroscopy (UV-Vis), Raman spectroscopy (RS), scanning electron microscopy (SEM), cyclic voltammetry (CV) and electrochemical impedance spectroscopy (EIS). UV-visible absorbance spectrum have indicated that the oxide have higher absorption of ultraviolet light compare to visible light. Raman spectroscopy confirm XRD data through no apparition of any impurity peak. The SEM image reveals a porous structure with nanoplaquettes coexisting with agglomerates of spherical grain size.

Copy Right, IJAR, 2017,. All rights reserved.

Introduction:-

Metal oxides nanoparticles such as $\text{Ni}_{0.9}\text{Co}_{2.1}\text{O}_4$ are used in different fields such as physical, chemical, electronic and biology due to their electrical, optical and photo-electrochemical properties. $\text{Ni}_{0.9}\text{Co}_{2.1}\text{O}_4$ and the other Ni-Co mixed oxides can be used as electrode materials in various applications such as oxygen evolution (Trassatti, 1991; Hu and Cheng, 1999) and reduction (Schumacher et al., 1990; Barakat, 2008), electrochromic devices (Barakat, 2008; Monk and Ayub, 1997;), lithium ion batteries (Larcher et al., 2002; Wang et al., 1999; Liu et al., 2008), supercapacitors (Hu and Cheng, 2002; Hosono et al., 2006; Srinivasan and Weidner, 2002), and protection film of cathodes in molten carbonate fuel cells (Pauporte et al., 2005; Mendoza et al., 2003; Mansour et al., 2006) . The properties of the metal nanoparticles depend on their sizes, shapes and composition (Amrut et al., 2010). The redox couples $\text{Ni}^{3+}/\text{Ni}^{2+}$ and $\text{Co}^{3+}/\text{Co}^{2+}$ present in the crystal structure provide notable electrocatalytic properties. Furthermore, the electronic conductivity of $\text{Ni}_{0.9}\text{Co}_{2.1}\text{O}_4$ has been reported to be much higher than those of nickel oxide and cobalt oxide (Dubal et al., 2015). Therefore, $\text{Ni}_{0.9}\text{Co}_{2.1}\text{O}_4$ is expected to show better catalytic properties compared to the single-component metal oxide due to rich redox reactions originating from Ni and Co cations present in different valence states (Srivastava et al., 2014). Metal oxide nanoparticles have variety of applications by their own. Thus, researches are going on to improve their properties and applications. The catalytic activity of catalysts is known to be highly rely on an electrochemically active surface area and the kinetic features of the

Corresponding Author:- Makhtar Guène.

Address:- Laboratoire de Chimie Physique Organique et d'Analyse Environnementale, Département de Chimie, Faculté des Sciences et Techniques, Université Cheikh Anta Diop, Dakar, Sénégal.

material. It can be enhanced by reducing the size and uniformly dispersing the nanoparticles, which can provide high surface area (Chang et al., 2010).

This field has prompted extensive research because it can provide clean and renewable energy sources, one of the major challenges in response to the needs of modern society and increased pollution. Water electrolysis is one of the most promising and most progressive methods of hydrogen (H_2) production. Hydrogen is expected to be one of the most promising energy sources in the future. Therefore, development of an electrocatalyst having high stability, high efficiency, low cost and low overpotential for oxygen and hydrogen evolution reaction is required. Keeping the above facts in mind, herein, we synthesized $Ni_{0.9}Co_{2.1}O_4$ by using sol-gel via propionic acid method and studied its morphological, optical and electrochemical properties and results of the study are presented in this paper.

Materials and Methods:-

2.1. Synthesis of $Ni_{0.9}Co_{2.1}O_4$

$Ni_{0.9}Co_{2.1}O_4$ nanostructured spinel oxide was prepared by the sol-gel method (Ponce et al., 1999). $Co(NO_3)_2 \cdot 6H_2O$, $Ni(NO_3)_2 \cdot 6H_2O$, and propionic acid were used as raw materials. Stoichiometric amounts of precursors were mixed according to the compound formula.

2.2. Physical characterization:

The morphology of $Ni_{0.9}Co_{2.1}O_4$ material was examined using a scanning electron microscopy (SEM, Hitachi model S-520). The Raman spectrum was recorded in the range of 200 - 800 cm^{-1} at room temperature using a Raman microscope Renishaw model 1000. The optical absorption spectrum of the mixed oxide powders is carried out at ambient temperature using a SAFAS 2000 UV-visible spectrophotometer whose spectral range extends over a range ranging from from 250 nm to 2000 nm.

2.3. Electrochemical characterization:

The cyclic voltammetry (CV) and electrochemical impedance spectroscopy (EIS) measurements were carried out at room temperature in a three-electrode glass cell in a solution of 3 M KOH aqueous electrolyte using a Potentiostat/Galvanostat Fra 2 μ Autolab Type III. A silver wire and an Hg/Hg_2Cl_2 (Saturated KCl) were used as the counter and reference electrodes, respectively. The oxide powder in a form of disk pastille (1.33 cm^2 surface area) were used as working electrode. The impedance spectra were recorded in a range of frequency from 10 kHz to 0.1 Hz by applying an AC voltage of 0.5 V.

2.4. Preparation of working electrode:

For electrodes with physical characteristics easily reproducible, with good electronic conductivity and good mechanical properties we were interested to rigid electrodes impregnated with electrolyte. They were made from a homogeneous mixture of cobalt and nickel mixed oxide as active material and a small amount of Teflon (5 wt %) which serves as a mechanical binder. Each of these components was weighed with an electronic balance. After weighing, the constituents were homogenized using a mortar and then introduced into a tableting mold of Beckam type of 13 mm diameter. A pressure of 3 ton / cm^2 (Touré et al., 1994) is applied to finally obtain pellet of 300 mg weight.

Results and discussions:-

3.1. Physical characterization of $Ni_{0.9}Co_{2.1}O_4$

3.1.1. Morphology of synthesized $Ni_{0.9}Co_{2.1}O_4$

Surface morphology of $Ni_{0.9}Co_{2.1}O_4$ oxide powders was studied with scanning electron microscopy. Fig. 1 shows the SEM images of $Ni_{0.9}Co_{2.1}O_4$ at two different magnifications. It is revealed from Fig. 1 (a & b), that $Ni_{0.9}Co_{2.1}O_4$ oxide powders are constituted of aggregates of grains in spherical shape with diameters up to around 1,6 μm , and nanoplates with lengths up to around 12 μm , an thickness of about 465 nm. Some singular spherical grains have also been observed in the morphology of the powders (Fig. 1b). The SEM micrographs also reveal that the samples have good dispersibility.

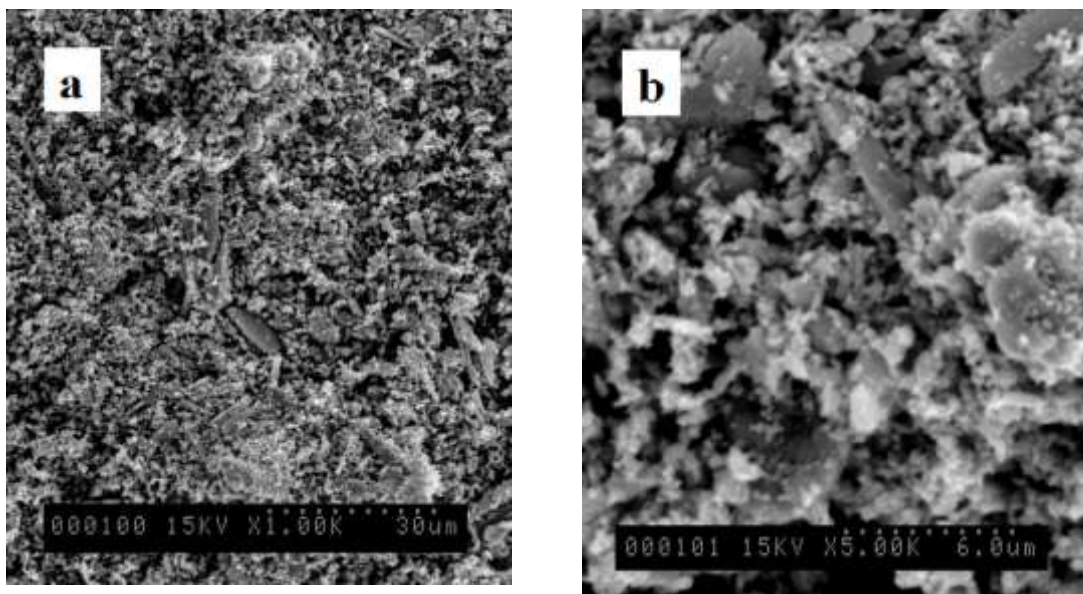


Fig 1:- SEM images of $\text{Ni}_{0.9}\text{Co}_{2.1}\text{O}_4$: (a) low magnification ; (b) high magnification

3.1.2. UV-vis analysis:

Figure III.3 gives the UV-vis spectrum of the mixed oxide $\text{Ni}_{0.9}\text{Co}_{2.1}\text{O}_4$ prepared by the sol-gel technique via propionic acid. The spectrum shows a higher absorbance of ultraviolet (UV) light relative to visible light, with a gradual increase in infrared absorption (> 800 nm) to the UV range (< 400 nm). The spectrum shows a broad absorption band at 250-550 nm with a maximum at $\lambda \approx 300$ nm. This band is attributed to Co (III) ions in tetrahedral sites (Guèye and Guène, 2015). The absence of a band above 550 nm is attributed to the replacement of Co ions by the Ni ions in the octahedral and tetrahedral sites, thus eliminating the orbital degeneration by adding new orbital energy levels (Gautier et al., 1997). Only a few previous studies on the optical properties of cobalt-based metal oxides have been carried out (Gautier et al., 1997, Windisch et al., 2001a, b; Nkeng et al., 1995).

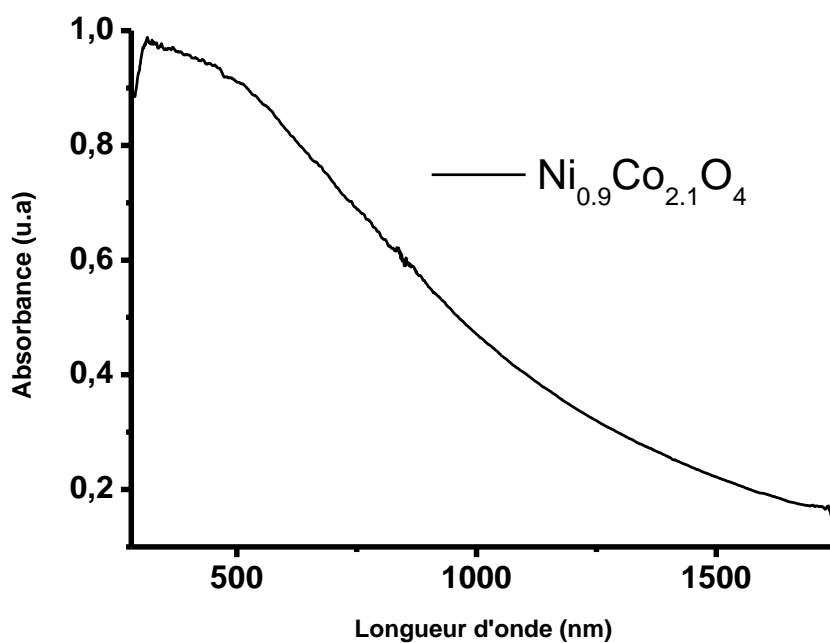


Fig. 2:- UV-vis. Spectrum of $\text{Ni}_{0.9}\text{Co}_{2.1}\text{O}_4$ synthesized by sol-gel method (propionic acid)

3.1.3. Raman studies:

Raman spectroscopy is used to obtain information on structural changes, composition and network disorders due to the substitution of Ni^{2+} ions in cobalt oxide. The Raman spectrum of the oxide $\text{Ni}_{0.9}\text{Co}_{2.1}\text{O}_4$ is shown in Figure III.4. The peaks observed at about 330, 465, 525 and 665 cm^{-1} correspond to the E_{2g} , E_g , F_{2g} and A_{1g} modes of $\text{Ni}_{0.9}\text{Co}_{2.1}\text{O}_4$, respectively (Ma et al., 2015; Jacintho et al., 2009). Only the Co-O and Ni-O vibrations of the oxide $\text{Ni}_{0.9}\text{Co}_{2.1}\text{O}_4$ were detected. No peaks corresponding to the OH group or another impurity (NiO for example) were observed, which implies that a pure oxide $\text{Ni}_{0.9}\text{Co}_{2.1}\text{O}_4$ was formed after calcination. These results are in good agreement with observations reported in the literature (Ma et al., 2015; Liu et al., 2013; Huang et al., 2013). They are also consistent with the results of DRX obtained above and confirm that the crystallographic structures of nickel and cobalt oxides can be identified by Raman spectroscopy.

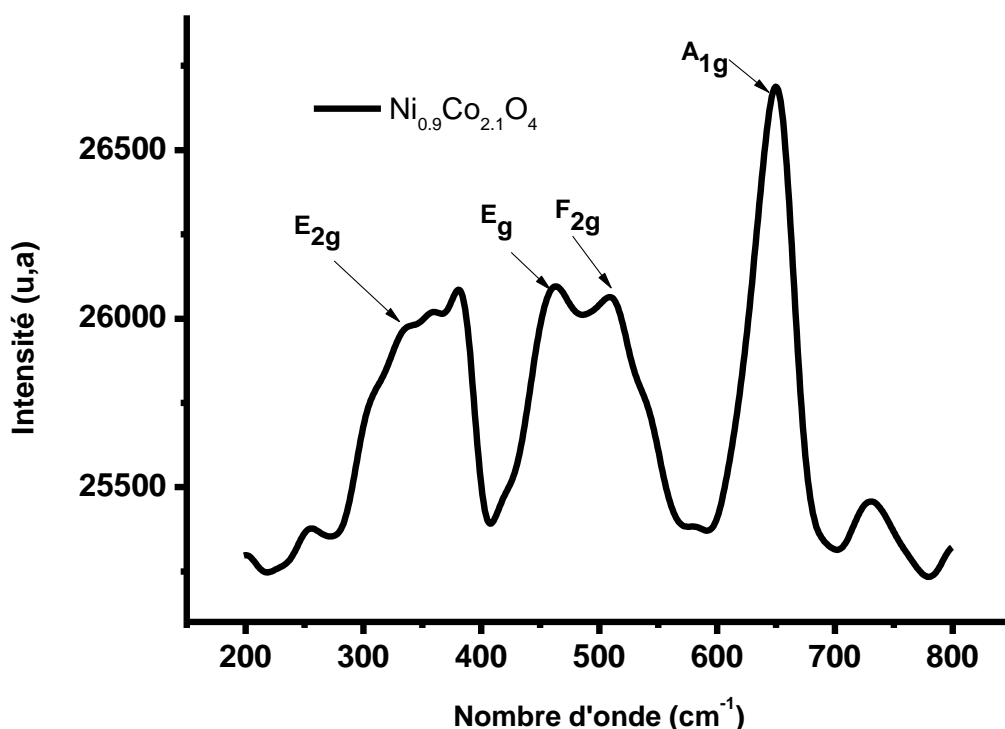


Fig. 3:- Raman Spectrum of $\text{Ni}_{0.9}\text{Co}_{2.1}\text{O}_4$ synthesized by sol-gel method (propionic acid)

3.2. Electrochemical properties of $\text{Ni}_{0.9}\text{Co}_{2.1}\text{O}_4$

3.2.1. Cyclic voltammetry

To investigate the electrochemical properties of the $\text{Ni}_{0.9}\text{Co}_{2.1}\text{O}_4$ electrode, cyclic voltammetry (CV) technique was used in a three-electrode system with Ag wire as counter electrode and a saturated calomel electrode (SCE) as reference electrode in 3 M KOH. Fig. 4a shows the CV curves of $\text{Ni}_{0.9}\text{Co}_{2.1}\text{O}_4$ electrode at different scan rates of 10, 20, 30, 40, 50, 60, 70, 80, 90 and 100 mV/s in the potential range of -0.5 to 0.1 (vs. SCE). The CV shape clearly reveals a pair of well-defined redox peaks in all curves, which is mainly attributed to the Faradic redox reactions. The anodic and the cathodic peaks are associated with the surface redox reactions of $\text{Co}^{2+}/\text{Co}^{3+}$ and $\text{Ni}^{2+}/\text{Ni}^{3+}$ solid redox state couple in the spinel nickel cobaltite (Huang et al., 2013; An et al., 2014; Wang et al., 2011; Yuan et al., 2012). When the scan rate increases from 10 to 100 mV/s , the current increases and the electrochemical polarization makes the redox peaks shift to more positive and negative directions, respectively. The shapes of the CV curves do not significantly changed with the increase of the scan rate, revealing the good electrochemical reversibility of the $\text{Ni}_{0.9}\text{Co}_{2.1}\text{O}_4$ electrode (Liu et al., 2012). Fig. 4b shows a good linear relationship of the currents of anodic and cathodic peaks versus the square of the scan rate, which indicate that the diffusion of the electrolyte ions OH^- is rate controlling process (Simon et al., 2014; Zhang et al., 2016).

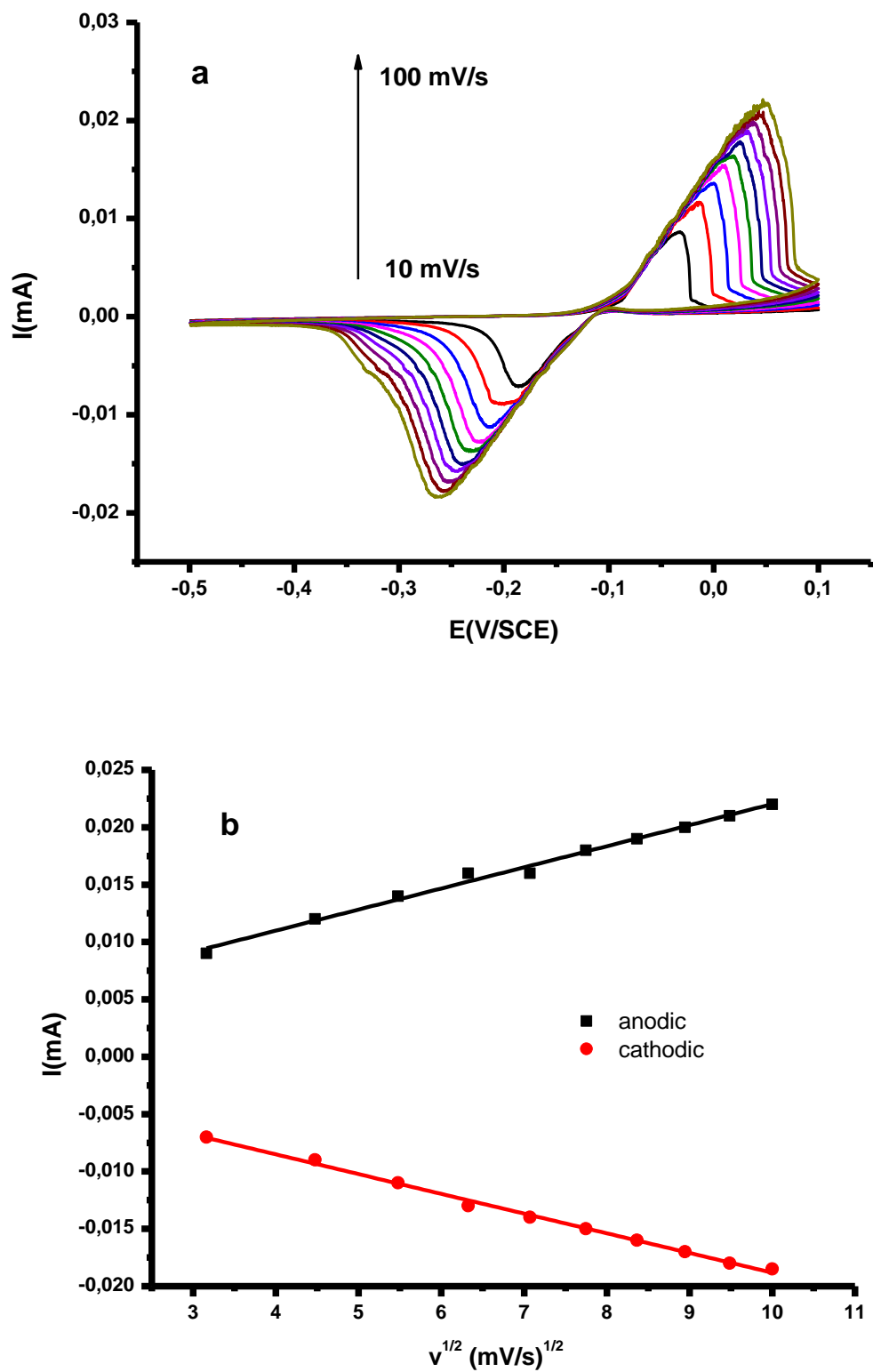


Fig. 4:- CV curves of $\text{Ni}_{0.9}\text{Co}_{2.1}\text{O}_4$ at different scan rates (a); relationship of the anodic and the cathodic peak currents versus square of the scan rate (b)

3.2.2. Electrochemical impedance spectroscopy (EIS):

The impedance spectrum of $\text{Ni}_{0.9}\text{Co}_{2.1}\text{O}_4$ was recorded in the frequency range 10 kHz to 100 mHz at a constant potential ($E = 0.5 \text{ V}$), in 3 M KOH solution. The Nyquist mode EIS for $\text{Ni}_{0.9}\text{Co}_{2.1}\text{O}_4$ in 3 M KOH is shown in Fig. 5. The plot consists of a depressed semicircle at high frequency region which diameter corresponds to the charge-transfer resistance (R_{ct}) of the electrode/electrolyte interface and, at low frequency, a sloping line which is associated with redox capacitive behavior of the spinel nickel cobaltite (Ma et al., 2015; Umeshbabu et al 2016). At the high frequency region, the intercept at the real axis represents the bulk resistance (R_s) of the electrochemical system (electrolyte resistance, intrinsic resistance of substrate, and contact resistance at the active material/current collector interface) (Umeshbabu et al 2016; Umeshbabu et al 2014; Lu et al., 2014). The finite slope of impedance spectrum in the lower frequency range is attributed to the Warburg impedance (Z_w), which is induced by the diffusion/transport of electrolyte ions within the pores of active material during the redox reactions. The line inclined at approximately 45° to the real axis (near vertical line) at low frequencies indicates capacitive behavior of the electrode (Umeshbabu et al 2016).

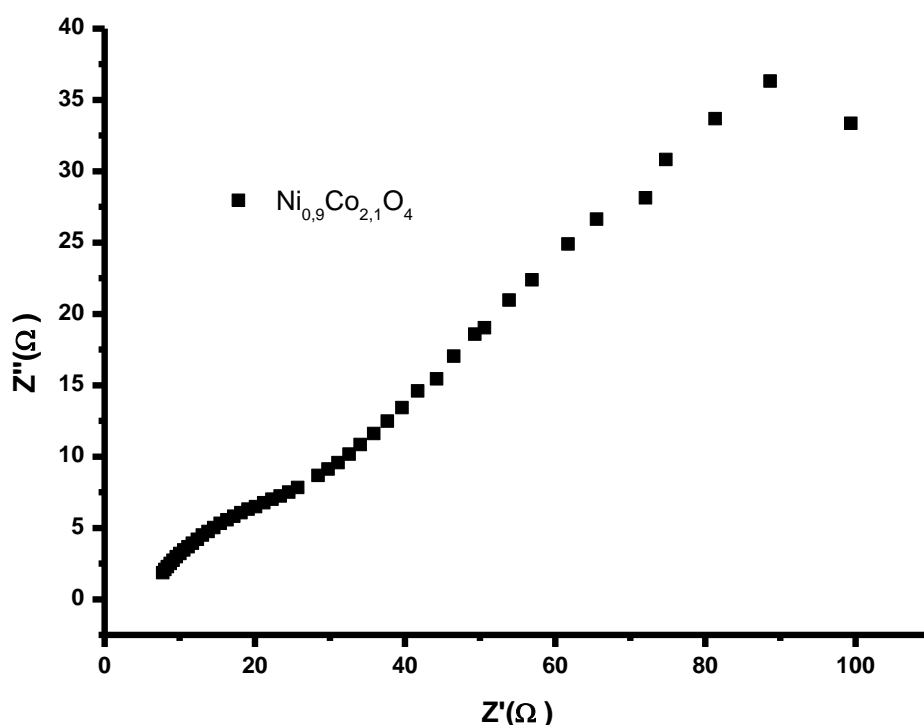


Fig. 5:- Impedance Nyquist plot of the $\text{Ni}_{0.9}\text{Co}_{2.1}\text{O}_4$ electrode.

Conclusion:-

$\text{Ni}_{0.9}\text{Co}_{2.1}\text{O}_4$ oxide was fabricated through a sol-gel via propionic acid method. The sample morphology of the oxide powders is constituted of aggregates of grains in spherical-like shape with good dispersibility. The UV-visible analysis reveals the presence of Co (III) cations in tetrahedral sites and the replacement of Ni ions by the Co ions in the octahedral and tetrahedral sites. The $\text{Ni}_{0.9}\text{Co}_{2.1}\text{O}_4$ electrode has good reversibility revealed by the cyclic voltammetry study, which also show that Faradic redox reactions associated with the surface redox reactions of $\text{Co}^{2+}/\text{Co}^{3+}$ and $\text{Ni}^{2+}/\text{Ni}^{3+}$. Furthermore, it is indicated that the diffusion of the hydroxide ions rate controlling process. EI-spectrum further exhibit enhanced capacitive behavior of the $\text{Ni}_{0.9}\text{Co}_{2.1}\text{O}_4$ electrode.

Acknowledgements:-

The authors would like to thank Pr M D Taylor, Anna Santoro, and Dr. Gramm. A. Ormondroyd of Bangor University in North Wales (U.K) for their support of this study.

References:-

1. Amrut, S. Lanje., Sathish, J. Sharma and Ramchandra, B. Pode. (2010): Magnetic and Electrical Properties of Nickel Nanoparticles prepared by Hydrazine Reduction Method. Scholars Research Library (Archives of Physics Research), Vol.1(1): pp. 49-56.
2. An, C., Wang, Y., Huang, Y., Xu, Y., Jiao, L., Yuan, H. (2014): Porous NiCo₂O₄ nanostructures for high performance supercapacitors via a microemulsion technique. Nano Energy, 10: 125-134.
3. Barakat, N. A. M., Khil, M. S., Sheikh, F. A., Kim, H. Y. (2008): Synthesis and Optical Properties of Two Cobalt Oxides (CoO and Co₃O₄) Nanofibers Produced by Electrospinning Process. J. Phys. Chem., C 112: 12225-12233.
4. Chang, K. H., Lee, Y. F., Hu, C. C., Chang, C. I., Liua, C. L., Yang, Y. L. (2010): A unique strategy for preparing single-phase unitary/binary oxides-graphene composites. Chem. Commun., 46: 7957-7959.
5. Dubal, D. P., Gomez-Romero, P., Sankapal, B.R., Holze, R. (2015): Nickel cobaltite as an emerging material for supercapacitors: An overview. Nano Energy, 11: 377-399.
6. Gautier, J. L., Trollund, E., Ríos, E., Nkeng, P., Poillierat, G. (1997): Characterization of thin CuCo₂O₄ films prepared by chemical spray pyrolysis. Study of their electrochemical stability by ex situ spectroscopic analysis. J. Electroanal. Chem., 428: 47-56.
7. Guèye, M and Guène, M. (2015): Structural Characterisation of Nickel - Cobalt Spinelrelated
8. Oxides of Ni_xCo_{3-x}O₄ (0 ≤ x ≤ 1.2) Prepared by Four Different Routes using XRD, FTIR, UV-vis-NIR and XPS. Ghana J. Sci., 55: 27-36.
9. Hosono, E., Fujihara, S., Honma, I., Ichihara, M., Zhou, H. (2006): Synthesis of the CoOOH fine nanoflake film with the high rate capacitance property. J. Power Sources, 158: 779.
10. Hu, C. C., Chen, C. A. (1999): Electrochemical characteristics of cobalt-based spinel oxides - I: Voltammetric behavior and O₂ evolution. J. Chin. Inst. Chem. Eng., 30: 431.
11. Hu, C. C., Cheng, C. Y. (2002): Ideally Pseudocapacitive Behavior of Amorphous Hydrous Cobalt-Nickel Oxide Prepared by Anodic Deposition. Electrochem. Solid-State Lett., 5: A43.
12. Huang, L., Chen, D., Ding, Y., Feng, S., Wang, Z. L., Liu, M. (2013): Nickel-Cobalt Hydroxide Nanosheets Coated on NiCo₂O₄ Nanowires Grown on Carbon Fiber Paper for High-Performance Pseudocapacitors. Nano Lett., 13: 3135-3139.
13. Jacintho, G.V.M., Brolo, A. G., Corio, P., Suarez, P. A. Z., Rubim, J. C. (2009): Structural investigation of MFe₂O₄ (M = Fe, Co) magnetic fluids. J. Phys. Chem., C 113: 7684-7691.
14. Larcher, D., Sudant, G., Leriche, J. B., Chabre, Y., Tarascon, J. M. (2002): The electrochemical reduction of Co₃O₄ in a lithium cell. J. Electrochem. Soc., 149: A234.
15. Liu, Q., Zhang, X., Yang, B., Liu, Jingyuan., Li, R., Zhang, H., Liu, L., and Wang, J. (2012): Construction of Three-Dimensional Homogeneous NiCo₂O₄ Core/Shell Nanostructure as High-Performance Electrodes for Supercapacitors. J. Electrochem. Soc., 162 (12): E319-E324.
16. Liu, Z.-Q. et al. (2013): Fabrication of hierarchical flower-like super-structures consisting of porous NiCo₂O₄ nanosheets and their electrochemical and magnetic properties. RSC Adv., 3: 4372-4380.
17. Liu, Y., Mi, C., Su, L., Zhang, X. (2008): Hydrothermal synthesis of Co₃O₄ microspheres as anode material for lithium-ion batteries. Electrochim. Acta., 53: 2507.
18. Lu, Y., Yan, H., Zhang, D., Lin, J., Xue, Y., Li, J., Luo, Y., Tang, C. (2014): Hybrid nanonet/nanoflake NiCo₂O₄ electrodes with an ultrahigh surface area for supercapacitors. J Solid. State Electrochem., 18: 3143-3152.
19. Ma, L., Shen, X., Zhou, H., Ji, Z., Chen, K., Zhu, G. (2015): High performance supercapacitor electrode materials based on porous NiCo₂O₄ hexagonal nanoplates/reduced graphene oxide composites. Chem. Eng. J., 262: 980-988.
20. Mansour, C., Pauporte, T., Ringuède, A., Albin, V., Cassir, M. (2006): Protective coating for MCFC cathode: Low temperature potentiostatic deposition of CoOOH on nickel in aqueous media containing glycine. J. Power Sources, 156: 23.
21. Mendoza, L., Albin, V., Cassir, M., Galtayries, A. (2003): Electrochemical deposition of Co₃O₄ thin layers in order to protect the nickel-based molten carbonate fuel cell cathode. J. Electroanal. Chem., 548: 95.
22. Monk, P. M. S., Ayub, S. (1997): Solid-state properties of thin film electrochromic cobalt-nickel oxide. Solid State Ionics, 99: 115.
23. Nkeng, P., Poillierat, G., Koenig, J. F., Chartier, P., Lefez, B., Lopitiaux, J., Lenglet, M. (1995): Characterization of Spinel-Type Cobalt and Nickel Oxide Thin Films by X-Ray Near Grazing Diffraction, Transmission and Reflectance Spectroscopies, and Cyclic Voltammetry. J. Electrochem. Soc., 142: 1777-1783.

24. Pauporte, T., Mendoza, L., Cassir, M., Bernard, M. C., Chivot, J. (2005): Direct Low-Temperature Deposition of Crystallized CoOOH Films by Potentiostatic Electrolysis. *J. Electrochem. Soc.*, 152: C49.
25. Ponce, J., Rios, E., Rehspringer, J. L., Poillerat, G., Chartier, P., Gautier, J. L. (1999): Preparation of Nickel Aluminum–Manganese Spinel Oxides $Ni_xAl_{1-x}Mn_2O_4$ for Oxygen Electrocatalysis in Alkaline Medium: Comparison of Properties Stemming from Different Preparation Methods. *J. Sol. State Chem.*, 145: 23.
26. Schumacher, L. C., Holzhueter, I., Hill, I. R., Dignam, M. J. (1990): Semiconducting and Electrocatalytic Properties of Sputtered Cobalt Oxide Films. *Electrochim. Acta*, 35: 975.
27. Simon, P., Gogotsi, Y., Dunn, B. (2014): Where do batteries end and supercapacitors begin? *Science Magazine*, 343: 1210–1211.
28. Srinivasan, V., Weidner, W. J. (2002): Capacitance studies of cobalt oxide films formed via electrochemical precipitation. *J. Power Sources*, 108: 15.
29. Srivastava, M., Uddin, M. E., Singh, J., Kim, N. H., Lee, J. H. (2014): Preparation and characterization of self-assembled layer by layer $NiCo_2O_4$ -reduced graphene oxide nanocomposite with improved electrocatalytic properties. *J. Alloys Compd.*, 590: 266-276.
30. Toure, M., Guene, M., Dieng, M. M., Lorquin, J. (1994): Environmental electrolytic influence in faradic capacity electrodes with p-naphthoquinone. Kinetic study of the redox reaction. *J. Islamic Acad Sci.*, 7(3): 175-180.
31. Trasatti, S. (1991) Physical electrochemistry of ceramic oxides. *Electrochim. Acta*, 36: 225.
32. Umeshbabu, E., Rajeshkhanna, G., Ranga Rao, G. (2014): Urchin and sheaf-like $NiCo_2O_4$ nanostructures: synthesis and electrochemical energy storage application. *Int. J. Hydrog. Energy*, 39: 15627–15638.
33. Umeshbabu, E., Rajeshkhanna, G., Ranga Rao, G. (2016): Effect of solvents on the morphology of $NiCo_2O_4$ /graphene nanostructures for electrochemical pseudocapacitor application. *J. Solid State Electrochem.*, 20 (7): 1837-1844.
34. Wang, H., Jang, Y. I., Huang, B., Sadoway, D. R., Chiang, Y. M. (1999): TEM study of electrochemical cycling-induced damage and disorder in $LiCoO_2$ cathodes for rechargeable lithium batteries. *J. Electrochem. Soc.*, 146: 473.
35. Wang, H., Gao, Q., Jiang, L. (2011): Facile Approach to Prepare Nickel Cobaltite Nanowire Materials for Supercapacitors. *Small*, 7: 2454.
36. Windisch Jr, C.F., Exarhos, G. J., Ferris, K. F., Engelhard, M. H., Stewart, D. C. (2001): Infrared transparent spinel films with p-type conductivity. *Thin Solid Films*, 398-399: 45-52.
37. Windisch, J.C.F., Ferris, K.F., Exarhos, G.J. (2001): in: The 47th international symposium:
38. Vacuum, thin films, surfaces/interfaces, and processing NAN06, AVS, Boston, Massachusetts
39. (USA), pp. 1647-1651.
40. Yuan, C., Li, J., Hou, L., Zhang, X., Shen, L., Lou, X. W. D. (2012): Ultrathin Mesoporous $NiCo_2O_4$ Nanosheets Supported on Ni Foam as Advanced Electrodes for Supercapacitors. *Adv. Funct. Mater.*, 22: 4592.
41. Zhang, X., Xiao, J., Zhang, X., Meng, Y., Xiao, D. (2016): Three-Dimensional Co_3O_4 Nanowires@Amorphous $Ni(OH)_2$ Ultrathin Nanosheets Hierarchical Structure for Electrochemical Energy Storage. *Electrochim. Acta*, 191: 758-766.